Original article

MOLECULAR METABOLISM

Thioesterase superfamily member 1 suppresses cold thermogenesis by limiting the oxidation of lipid droplet-derived fatty acids in brown adipose tissue

Kosuke Okada [1], Katherine B. LeClair [1], Yongzhao Zhang [1,4], Yingxia Li [1], Cafer Ozdemir [1], Tibor I. Krisko [1], Susan J. Hagen [2], Rebecca A. Betensky [3], Alexander S. Banks [1], David E. Cohen [1,*]

ABSTRACT

Objective: Non-shivering thermogenesis in brown adipose tissue (BAT) plays a central role in energy homeostasis. Thioesterase superfamily member 1 (Them1), a BAT-enriched long chain fatty acyl-CoA thioesterase, is upregulated by cold and downregulated by warm ambient temperatures. *Them1*$^{-/-}$ mice exhibit increased energy expenditure and resistance to diet-induced obesity and diabetes, but the mechanistic contribution of Them1 to the regulation of cold thermogenesis remains unknown.

Methods: *Them1*$^{-/-}$ and *Them1*$^{+/+}$ mice were subjected to continuous metabolic monitoring to quantify the effects of ambient temperatures ranging from thermoneutrality (30 °C) to cold (4 °C) on energy expenditure, core body temperature, physical activity and food intake. The effects of Them1 expression on O_2 consumption rates, thermogenic gene expression and lipolytic protein activation were determined *ex vivo* in BAT and in primary brown adipocytes.

Results: Them1 suppressed thermogenesis in mice even in the setting of ongoing cold exposure. Without affecting thermogenic gene transcription, Them1 reduced O_2 consumption rates in both isolated BAT and primary brown adipocytes. This was attributable to decreased mitochondrial oxidation of endogenous but not exogenous fatty acids.

Conclusions: These results show that Them1 may act as a break on uncontrolled heat production and limit the extent of energy expenditure. Pharmacologic inhibition of Them1 could provide a targeted strategy for the management of metabolic disorders via activation of brown fat.

Keywords Energy expenditure; Fatty acyl-CoA; Acyl-CoA thioesterase; Mitochondria; Obesity

1. INTRODUCTION

In response to cold exposure, activation of mitochondria-rich brown adipose tissue (BAT) by norepinephrine (NE) signaling promotes non-shivering thermogenesis [1]. Heat is generated when mitochondrial β-oxidation is uncoupled from oxidative phosphorylation by uncoupling protein 1 (Ucp1). Key events include the liberation of intracellular triglycerides from lipid droplets by activation of lipolysis. The released free fatty acids (FFA) are channeled to mitochondria following their conversion to fatty acyl-CoAs by long chain acyl-CoA synthetase (Acsl) 1 [2].

Cold exposure also leads to transcriptional upregulation of a thermogenic gene profile in BAT [3,4]. Thioesterase superfamily member (Them) 1 (synonyms: brown fat inducible thioesterase (BFIT), steroidogenic acute regulatory protein-related lipid transfer (START) domain 14 (StarD14)/acyl-CoA thioesterase 11 (Acot11)) was identified as a BAT-enriched gene that was upregulated when mice were exposed to cold and was suppressed by acclimation to warm ambient temperatures [5]. Them1 is a type 2 acyl-CoA thioesterase [6,7], and the recombinant protein catalyzes the hydrolysis of long chain fatty acyl-CoA molecules into FFA plus CoASH [8,9]. Based on its transcriptional upregulation in concert with thermogenesis and higher

[1]Department of Medicine, Brigham and Women's Hospital, Harvard Medical School, Boston, MA, USA [2]Department of Surgery, Beth Israel Deaconess Medical Center, Harvard Medical School, Boston, MA, USA [3]Department of Biostatistics, Harvard T.H. Chan School of Public Health, Boston, MA, USA

[4] Present address: Envirologix, Inc., 500 Riverside Industrial Pkwy, Portland, ME 04103, USA.

*Corresponding author. Brigham and Women's Hospital, 77 Avenue Louis Pasteur, HIM 941, Boston, MA 02115, USA. Tel.: +1 (617) 525 5090; fax: +1 (617) 525 5100. E-mail: dcohen@partners.org (D.E. Cohen).

Abbreviations: Acot, acyl-CoA thioesterase; Ascl, long chain acyl-CoA synthetase; Atgl, adipose triglyceride lipase; AUC, area under the curve; BAT, brown adipose tissue; ASM, acid soluble metabolites; BFIT, brown fat inducible thioesterase; CPT, carnitine palmitoyl transferase; Fabp, fatty acid binding protein; FCCP, carbonyl cyanide-p-trifluoromethoxyphenylhydrazone; FFA, free fatty acids; Hsl, hormone sensitive lipase; PKC, protein kinase C; Plin, perilipin; MOI, multiplicity of infection; NE, norepinephrine; OCR, oxygen consumption rate; Ppar, peroxisome proliferator-activated receptor; RER, respiratory exchange rate; START, steroidogenic acute regulatory protein-related lipid transfer; Them1, thioesterase superfamily member; UCP, uncoupling protein; WAT, white adipose tissue

Received February 1, 2016 • Revision received February 9, 2016 • Accepted February 12, 2016 • Available online 23 February 2016

http://dx.doi.org/10.1016/j.molmet.2016.02.002

expression in BAT of obesity resistant mouse strains, it has been postulated that Them1 promotes energy expenditure [5,10]. However, *Them1*$^{-/-}$ mice exhibit increased energy expenditure at room temperature, along with resistance to high fat diet-induced obesity and glucose intolerance, suggesting that Them1 may instead limit the thermogenic capacity of BAT [11]. Although the mechanism is unknown, reduced acyl-CoA thioesterase activities of BAT homogenates from *Them1*$^{-/-}$ mice taken together with increased tissue concentrations of long chain fatty acyl-CoAs suggest that Them1 functions endogenously as a fatty acyl-CoA thioesterase [9,11]. This study examined Them1-mediated regulation of energy expenditure when mice were challenged with cold stress and the mechanism responsible for this effect. The results demonstrate that Them1 in BAT suppresses non-shivering thermogenesis by limiting the oxidation of lipid droplet-derived fatty acids. We propose that Them1 in BAT directly regulates the availability of substrates to be utilized for β-oxidation and uncoupling.

2. METHODS

2.1. Animals and diets

Male 5 to 13 w-old *Them1*$^{-/-}$ and littermate *Them1*$^{+/+}$ mice [11] were housed in a barrier facility with free access to water and a standard chow diet (PicoLab Rodent Diet 20, 5053, LabDiets; St. Louis, MO, USA). The ambient temperature was maintained at 22 ± 1 °C and the light and dark cycles were each 12 h (light cycle: 6 AM–6 PM, dark cycle: 6 PM–6 AM). Body composition was determined by NMR spectroscopy using an EchoMRI 3-in-1 Body Composition Analyzer (Houston, TX, USA). For experiments designed to measure core body temperature, mice were surgically implanted with small intraperitoneal temperature transponders (Mini Mitter, Bend, OR, USA) as previously described [12], and allowed a 1 w recovery period prior to experiments. In order to harvest tissue and plasma, mice were fasted for 4 h and then euthanized using CO_2. Samples were snap-frozen in liquid nitrogen and stored at −80 °C. All protocols for animal use and euthanasia were approved by the institutional committee of Harvard Medical School.

2.2. Comprehensive mouse monitoring

Experiments were performed using a temperature- and light (12 h light/dark cycle)-controlled Comprehensive Lab Animal Monitoring System (CLAMS, Columbus Instruments; Columbus, OH, USA) essentially as described [12]. Briefly, 9–12 w-old mice were placed in individual cages without bedding, but with free access to chow and water. Rates (ml/kg/h) of O_2 consumption (VO_2) and CO_2 production (VCO_2), as well as core body temperatures were determined at 11 min intervals. Respiratory exchange ratio (RER) values were calculated as VCO_2/VO_2. Rates of energy expenditure (kJ/h) were calculated from gas exchange. Activity was determined according to beam breaks and food intake was measured gravimetrically.

Each mouse was weighed prior to being placed in the CLAMS. Mice were studied at ambient temperatures ranging from 30 °C to 4 °C according to two different experimental designs [12]. Under "temperature-dynamic conditions", mice were first acclimated to 30 °C for 24 h in the CLAMS prior to 24 h of data recording. The ambient temperature was then reduced sequentially every 24 h. Data were recorded continuously, without further acclimation periods. During the course of these experiments, mice were not removed from their cages to determine temperature-dependent body weights and compositions, which were instead calculated based on the initial weights of the mice and average temperature-dependent rates of weight loss and body compositions determined in separate experiments. For "temperature-equilibrated" conditions, mice were housed for 96 h at each ambient temperature, with 48 h for acclimation, and then 48 h for data collection. Body weights and composition were determined at the beginning and end of exposure to each ambient temperature and averaged to yield values for each recording period. Because mice implanted with metal-containing temperature transponders could not be subjected to NMR determinations of body composition, separate cohorts of mice were utilized for determinations of core body temperature.

For each ambient temperature, cumulative values of energy expenditure were adjusted for differences in lean body weight and compared by analysis of covariance (ANCOVA) [12,13] using VassarStats (www.vassarstats.net). We fit separate linear mixed effects regression models for rates of energy expenditure at each ambient temperature for the temperature-dynamic experiments and the temperature-equilibrated experiments. Random effects were included for mice to adjust for correlation within groups, and fixed effects for genotype, lean body weight, dark versus light and the interaction of genotype with dark versus light. Least squares means estimates of rates of energy expenditure were calculated for each genotype and dark/light combination to adjust for lean body weight. Similar mixed effects models were fit for core body temperature, total activity and ambulatory activity, without adjustment for lean body weight. SAS Version 9.3 (SAS Institute Inc., Cary, NC, USA) was utilized to implement these analyses.

In a separate experiment, mice were acclimated to 30 °C overnight in the CLAMS. VO_2 values were then recorded for 120 min, after which mice were injected (0.5 mg/kg) with the selective β_3-adrenergic receptor agonist CL316,243 (Sigma Chemical Co. St Louis, MO, USA) [14]. Mice were returned immediately to the CLAMS and values of VO_2 recorded for an additional 280 min. To measure the response of BAT gene expression to CL316,243, similarly treated mice were sacrificed 60 or 90 min following injection. For gene expression studies, mice injected with an equal volume of PBS and sacrificed after 90 min served as controls.

2.3. Surface infrared thermography

Thermal radiation was assessed in mice housed for 48 h at ambient temperatures ranging from 30 °C to 4 °C using an FLIR Systems model T420 infrared camera (Wilsonville, OR, USA) as described [15], with minor modifications. To eliminate stray light, the FLIR camera was mounted on a box and placed over a custom-designed metal grid at focal length of 30 cm. Immediately upon removal from their temperature-controlled environment, mice were anesthetized with isoflurane and then placed in the prone position on the metal grid. Separate images were taken of the back and the tail. To enable specific imaging of the proximal tail, handling of mice was limited to the distal-most tip of the tail, which was placed on a dark felt support. Thermal images were captured at emissivity setting of 0.95 in JPG format. Images were converted to semicolon-delimited. CSV files using the FLIR ResearchIR program. Files were then batch converted to RAW format using Matlab (The Mathworks, Natick, MA, USA) (*script kindly provided by J. Crane & G. Steinberg, Macmaster Univ., Ottowa, Ontario, Canada*), which were imported into AMIDE image analysis software (http://www.amide.sourceforge.net) with the following specified format: "float, little endian 32-bit," 0 offset bytes, 240 × 320 × 1 dimensions (specific to the camera model) with gate, frames and voxel size each set to 1. For interscapular or tail imaging, digital fiducial markers were placed at the midline and rearward base of the ears or base of tail, respectively, and referenced to align and overlap each image. For the interscapular area, the region of interest (ROI) was placed as 24.5 mm aligned with the long axis of mouse × 28.0 mm beginning at the rearward base of the ears and centered on the

scapulae. For the tail, a ROI 24.0 mm × 50.8 mm was placed over the tail, beginning at its base and centered on the long axis of the tail. Absolute scaling of the ROI was confirmed using the custom-designed grid spacing. For each ROI, the mean of the warmest 10% of voxels was calculated using Amide and designated to be the thermal radiation value for the sample.

2.4. Biochemical analyses

Concentrations of FFA and triglycerides in tissue, cells and plasma were determined using reagent kits (Wako Chemicals; Richmond, VA, USA). Plasma glycerol concentrations were determined using a free glycerol determination kit (Sigma—Aldrich; St. Louis, MO). Plasma glucose concentrations were determined using a OneTouch Ultra glucose monitor (LifeScan, Inc.; Milpitas, CA, USA).

2.5. Histology and ultrastructure

Freshly harvested BAT from 12 to 13 w-old mice was immersed in Bouin's fixative solution. Hematoxylin and eosin staining was performed by the Histology Core at the Beth Israel Deaconess Medical Center, Harvard Medical School, Boston, MA. Electron microscopy was performed as previously described [12]. Following fixation, dehydration, and embedding in LX112 resin (Ladd Research Industries; Burlington, VT), ultrathin BAT sections were prepared using a Leica Ultracut E ultramicrotome (Leica Microsystems; Deerfield, IL). These were visualized with a JEOL 1400 electron microscope (JEOL USA: Peabody, MA, USA), and images taken using with a GatanCCD camera (Gatan; Warrendale, PA, USA).

2.6. Culture and differentiation of primary brown adipocytes

Primary brown preadipocytes were isolated, cultured, and then differentiated as described [12]. Briefly, BAT harvested from 5 to 7 w-old mice ($n = 7$/group) was pooled, minced, digested with collagenase (Sigma—Aldrich) and dispersed in DMEM containing 4.5 g/L glucose, 0.1 mM pyruvate, 10 mM HEPES, 1% penicillin-streptomycin and 1 μg/ml fungizone. Unless otherwise specified, media contained 10% FBS. After 5—6 d, cells were trypsinized and seeded at 25,000 cells/cm^2. When cells achieved confluence, differentiation of the preadipocytes was initiated by addition to the media of 1 μM rosiglitazone (Sigma—Aldrich) for 7 d [16]. This method was chosen because preliminary experiments revealed greater Them1 and Ucp1 expression than observed using the combination of isobutylmethylxanthine, dexamethasone, and indomethacin [17]. In selected experiments, the media was supplemented with L-(−)-norepinephrine-(+) bitartrate (NE, Calbiochem, EMD Millipore; Billerica, MA, USA), palmitate or oleate (Sigma—Aldrich) conjugated with fatty acid-free BSA [18], 300 nM of the pan protein kinase C (PKC) inhibitor phorbol 12-myristate 13-acetate (PMA) (LC Laboratories; Woburn, MA, USA) [19] or 100 μM H_2O_2 (Sigma—Aldrich) [20] and replenished daily from d3—d7 of differentiation.

Heterologous protein expression in primary brown adipocytes was achieved using recombinant adenovirus. The open reading frame of Them1 was cloned into VQAd5-CMV (ViraQuest; North Liberty, IA, USA) along with an N-terminal FLAG-tag downstream of the CMV promoter. This was used to create the Them1 adenovirus (Ad-Them1) by standard techniques (ViraQuest). A recombinant GFP adenovirus (Ad-GFP, ViraQuest), as well as Ad-Them2 [18] were used as controls. Recombinant adenoviruses were added to the medium for 24 h during d1 of differentiation.

2.7. O_2 consumption rates (OCR)

The O_2 consumption rate (OCR) of BAT were measured *ex vivo* using a Clark electrode YSI 5300A Biological Oxygen Monitor System (YSI Life Sciences; Yellow Springs, OH, USA). BAT was isolated from male 7—9 w-old mice after exposure to ambient temperatures of 22 °C or 4 °C for 96 h. For duplicate measurements, BAT was separated into two pieces, which were weighed separately. Immediately upon harvesting, tissues were minced finely and suspended (50—70 mg BAT per 3 ml) in unbuffered DMEM media containing 25 mM glucose, 10 mM sodium pyruvate and 2 mM GlutaMAX (Life Technologies; Carlsbad, CA) in the 2 separate temperature-controlled chambers of the apparatus. Time-dependent values of [O_2] were determined for 5 min at 37 °C. OCR values (%/min) were determined by fitting to the equation [O_2] (% initial concentration) $= 100{*}e^{-OCR{*}t}$. OCR for an individual BAT sample was determined as the average of duplicate values. Values of OCR were adjusted for differences in BAT weight by ANCOVA using VassarStats. OCR values were measured in primary brown adipocytes using an XF24 extracellular flux analyzer (Seahorse Bioscience; North Billerica, MA, USA). Primary brown adipocytes were seeded at 25,000 cells/cm^2 in customized Seahorse 24-well plates (Seahorse Bioscience) and differentiated as described above. Mature brown adipocytes were incubated in the absence of CO_2 for 1 h at 37 °C in Krebs—Henseleit buffer (pH 7.4) containing 0.45 g/L glucose, 111 mM NaCl, 4.7 mM KCl, 2 mM $MgSO_4$-$7H_2O$, 1.2 mM Na_2HPO_4, 5 mM HEPES and 0.5 mM carnitine (Sigma—Aldrich). OCR values were measured before and after the exposure of cells to NE, etomoxir (Sigma—Aldrich), Atglistatin (EMD Millipore) or palmitate (Sigma—Aldrich) conjugated with fatty acid-free BSA [18]. To determine the acute responses of OCR to NE, etomoxir or Atglistatin, 300 μl Krebs—Henseleit buffer was added to the medium (total 560 μl). To determine the acute response of OCR to palmitate, the culture medium was changed to 560 μl Krebs—Henseleit buffer. NE, FFA, Atglistatin and etomoxir were each dissolved in 75 μl Krebs—Henseleit buffer and added to the total 560 μl of medium from the injection ports of the Seahorse apparatus.

To test mitochondrial respiratory function, the culture medium was changed to unbuffered DMEM media containing 25 mM glucose, 10 mM sodium pyruvate and 2 mM glutamax. The ATP synthase inhibitor, oligomycin, the mitochondrial uncoupler carbonyl cyanide-p-trifluoromethoxyphenylhydrazone (FCCP), the electron transfer inhibitor, rotenone and antimycin A (Seahorse) were sequentially added to each well [18]. OCR values are represented either as pmol/min/mg of protein or as the percentage of change when compared with basal OCR values.

2.8. Rates of lipolysis

NE-induced lipolysis was measured in mature primary brown adipocytes by measuring glycerol released into culture media using a free glycerol determination kit (Sigma—Aldrich) as described [12]. Briefly, fully differentiated primary brown adipocytes were incubated for 1 h in phenol red-free non-buffered DMEM (Sigma—Aldrich) containing 2% fatty acid-free bovine serum albumin (Sigma—Aldrich). The media were then replaced by fresh media plus 1 μM NE. The media were sampled periodically during a 3 h incubation period to determine glycerol concentrations. Data were normalized to cellular protein contents.

2.9. Fatty acid oxidation rates

Rates of fatty acid oxidation were determined in primary brown adipocytes according to the conversion of [1—^{14}C] palmitate (55 mCi/mmol: American Radiolabeled Chemicals; St. Louis, MO, USA) into ^{14}C-acid soluble metabolites (ASM) and -CO_2 [18]. Briefly, matured brown adipocytes were incubated for 6 h in 2 ml of fresh culture medium with 10% FBS supplemented with 1 mM carnitine (Sigma—Aldrich) and 0.25 μCi [1—^{14}C] palmitate/ml plus 200 μM palmitate conjugated with

fatty acid-free BSA. To determine ASM, the culture medium was mixed in conical tubes with 200 μl of 70% perchloric acid (Fisher Scientific; Pittsburgh, PA, USA) with filter papers soaked in 2N NaOH placed in the caps in order to trap $^{14}C-CO_2$. After incubation for 1 h on a horizontal shaker, the filter papers were removed, and the acidified medium was incubated overnight at 4 °C and then centrifuged at 14,000 × g for 20 min ^{14}C-labeled CO_2 in the filter paper and ASM in the supernatant were dissolved in Ecoscint H (National Diagnostics; Atlanta, GA, USA) and were counted using a LS6000IC liquid scintillation counter (Beckman Coulter; Danvers, MA).

2.10. Immunoblot analysis

Tissue and cells were homogenized in RIPA buffer (1% Nonidet P-40, 0.1% sodium deoxycholate, 0.1% SDS, 150 mM NaCl, 50 mM Tris—HCl, 2 mM EDTA) for determination of protein expression by immunoblot analysis. Protein concentrations were determined spectrophotometrically using a Bio-Rad protein assay dye reagent, and equal amounts of proteins separated by SDS-PAGE. Following electrophoretic transfer to nitrocellulose membranes (GE Healthcare; Pittsburgh, PA, USA), blots were probed with specific primary antibodies: Antibodies to Them1 and β-Actin were as described previously [11]. Antibodies to Ucp1 and adipose triglyderide lipase (Atgl) were obtained from Abcam (Cambridge, MA, USA). Antibodies to hormone sensitive lipase (Hsl) and phospho- Hsl were from Cell Signaling Technology, and antibodies to perilipin 1 (Plin1) from Fitzgerald Industries (Acton, MA, USA). Primary antibodies were detected by enhanced chemiluminescence (SuperSignal West DURA, Fisher).

2.11. Statistics

Differences were evaluated using two-tailed unpaired Student's *t*-tests when two groups were compared. Multiple group comparisons were performed using two-way ANOVA. Differences were considered significant for $P < 0.05$.

3. RESULTS

3.1. Enhanced cold thermogenesis in Them1-deficient mice

We tested the regulatory role of Them1 in cold thermogenesis using two experimental designs (Figure 1A,B, S1 and Table S1) in order to assess: 1) the acute response to exposures of mice to cold stress (referred to here as "temperature-dynamic"), and 2) the equilibrated response to prolonged exposures (referred to here as "temperature-equilibrated"). We have previously demonstrated that these responses may differ substantially as mice acclimate to changes in ambient temperature [12]. Daily energy expenditures were calculated from hourly rates (Figure S1A and B), which were then adjusted for lean body weights (Figure S1E and F). In *Them1*$^{-/-}$ mice, daily energy expenditure levels were increased at ambient temperatures of 22 °C or lower under temperature-dynamic conditions (Figure 1A) and at 4 °C under temperature-equilibrated conditions (Figure 1B). At 4 °C, *Them1*$^{-/-}$ mice had greater total daily energy expenditures under both temperature-dynamic and temperature-equilibrated conditions. Greater energy expenditures were also frequently observed during the light phase. At the thermoneutral ambient temperature of 30 °C, increases in energy expenditure during the light phase in *Them1*$^{-/-}$ mice most likely reflected incomplete acclimation to the warm temperature since these mice were chronically housed at 22 °C [21].

For *Them1*$^{-/-}$ mice under temperature-dynamic conditions, significant increases in adjusted mean hourly rates of energy expenditure were observed at ambient temperatures of 22 °C and below (Table S1). Under temperature-equilibrated conditions, the increases in mean hourly rates of energy expenditure were smaller in magnitude and did not themselves achieve statistical significance (Table S1). There were no systematic effects of Them1 expression on core body temperatures (Figure S1C and D, and Table S1), food intake (Figure S1G and H) or either daily or hourly physical activities (Figures S1I—L and Table S1). Increased rates of energy expenditure in *Them1*$^{-/-}$ mice could have resulted from changes in heat loss in response to alterations in vasomotor tone or skin lipid composition [22]. However, we did not observe evidence of genotype-dependent differences in heat dissipation determined by surface infrared thermography as functions of ambient temperature (Figure S1M—P).

Although Them1 is highly enriched in BAT, our use of a global Them1-deficient mouse model leaves open the possibility that Them1 could be acting to suppress energy expenditure by an alternative mechanism. To address this issue, we measured rates of VO_2 in response to the specific β_3-receptor agonist CL316,243 in mice housed at thermoneutrality (Figure 1C—E) [14,23]. Under these conditions, baseline values of VO_2 were similar in *Them1*$^{+/+}$ and *Them1*$^{-/-}$ mice. Acute β_3-induced increases in VO_2 occurred similarly in both genotypes. However, VO_2 values declined much more slowly in the absence of Them1 expression (Figure 1C). Whereas this occurred in the absence changes in Them1 mRNA (Figure 1D), the responses of thermogenic genes to CL316,243 injection were largely preserved in *Them1*$^{-/-}$ mice (Figure 1E).

Histology of BAT sections revealed qualitative reductions in lipid droplet size and abundance in *Them1*$^{-/-}$ mice, which were more pronounced at 4 °C (Figure 2A). This was validated by BAT triglyceride and FFA concentrations, which were also reduced more markedly in *Them1*$^{-/-}$ mice at 4 °C (Figure 2B). These changes were not accompanied by alterations in BAT ultrastructure, as evidenced by electron microscopy, which demonstrated typical appearing lipid droplets and mitochondria in both genotypes (Figure 2A).

In plasma (Figure 2C), triglyceride concentrations were reduced by housing mice at 4 °C, but unaffected by Them1 expression. Plasma FFA and glycerol concentrations in *Them1*$^{-/-}$ mice were increased at 22 °C, but were not significantly higher at 4 °C. These changes in steady state plasma concentrations suggest greater triglyceride turnover due to increased demand for energy substrates by BAT. By contrast, plasma glucose concentrations were decreased in the absence of Them1 both at 22 °C and 4 °C. As previously reported [11], *Them1*$^{-/-}$ mice exhibited more rapid clearance of exogenously administered glucose and increased clearance rates of glucose during insulin tolerance tests, suggesting that decreased plasma glucose concentrations were attributable to greater glucose utilization, presumably by BAT of *Them1*$^{-/-}$ mice. Indeed, the absence of appreciable changes in RER values (Table S1) supports the likelihood that consumption of both fatty acids and glucose as energy substrates was increased by the absence of Them1 in BAT.

3.2. Increased O_2 consumption in Them1-deficient BAT *ex vivo*

To further localize the effects of Them1 on energy expenditure, we examined O_2 consumption in BAT *ex vivo* in response to a cold challenge. Compared with mice housed at 22 °C, expression of Them1 (Figure 3A,B) and Ucp1 (Figure 3A,C) in BAT were both increased by exposure to 4 °C. More prolonged 96 h exposure to 4 °C was associated with further upregulation of Them1 protein, but with no further increase in mRNA expression. There was no influence of Them1 expression on Ucp1 expression. In contrast to BAT, there was no influence of ambient temperature on Them1 expression in epididymal or inguinal white adipose tissue (WAT) tissue or in liver (Figure S2A). Ucp1

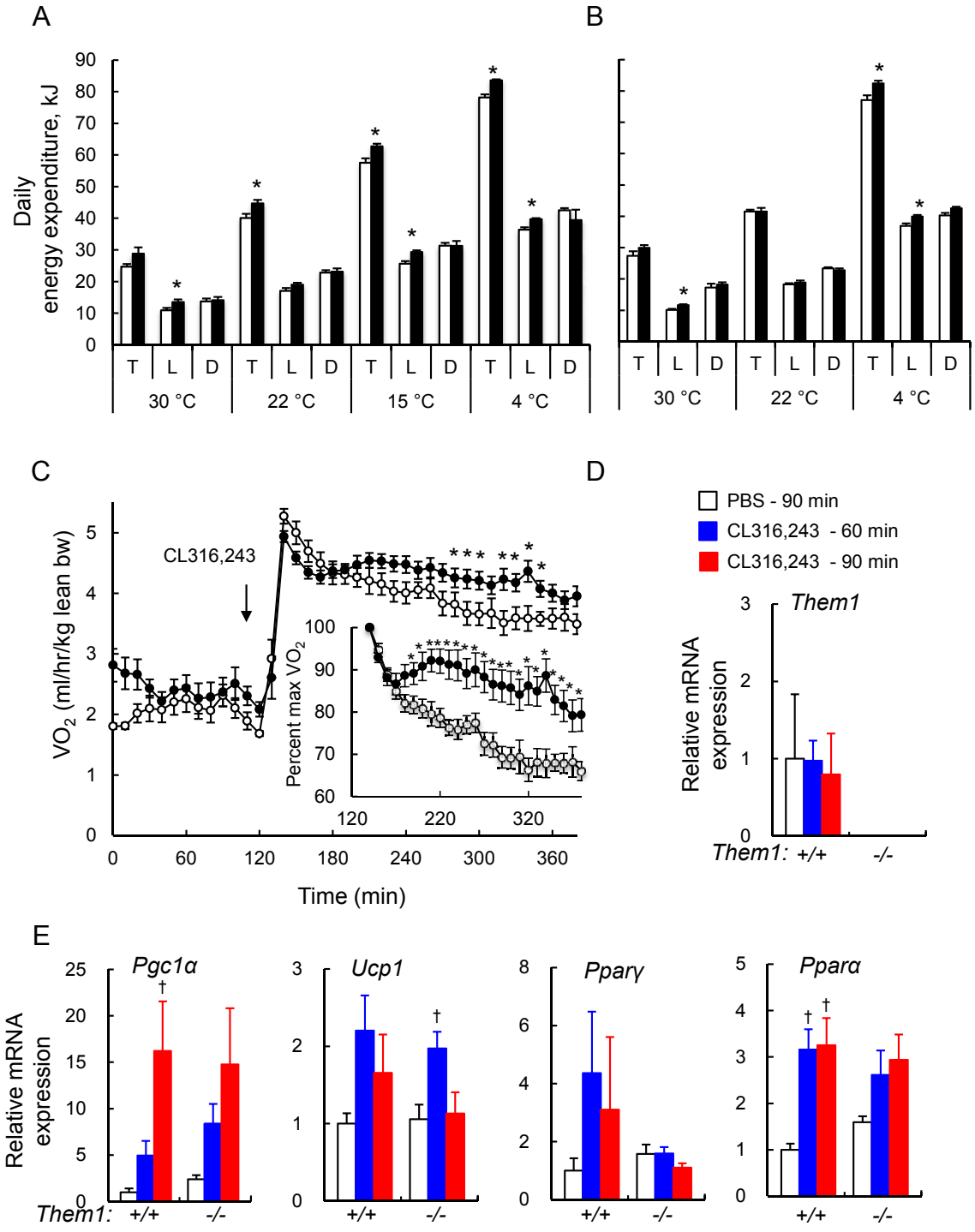

Figure 1: Them1 suppresses energy expenditure in response to thermal stress in mice. For mice (n = 6/group) housed under (A) temperature-dynamic and (B) temperature-equilibrated conditions, daily values of total (T) energy expenditure as well as the 12 h light (L) and dark (D) phases. For mice under temperature-equilibrated conditions (B), values of energy expenditure represent averages of the 2 diurnal cycles. (C) Response to CL316,243 (0.5 mg/kg) of VO_2 values for mice housed at 30 °C (n = 9/group). The inset panel shows data normalized to maximum VO_2 values following CL316,243 injection, which did not differ between genotypes. Relative expression of mRNA in BAT of mice housed at 30 °C (n = 3/group) for (D) Them1 and (E) thermogenic genes following injection of CL316,243 or PBS. Error bars represent ± SEM. $^{*}P < 0.05$, *Them1*$^{-/-}$ vs. *Them1*$^{+/+}$ mice; $^{\dagger}P < 0.05$, CL316,243 vs. PBS.

expression in inguinal WAT was not influenced by absence of Them1 expression (Figure S2A).

Ratios of interscapular BAT to total body weight were increased by 96 h exposure to 4 °C, but this was not influenced by Them1 expression (Figure 3D). The OCR in BAT was more rapid for mice housed at 4 °C than at 22 °C (Figure 3E), and at each temperature, the absence of Them1 expression increased the rate of decline. Because values of OCR varied linearly as functions of excised BAT mass (Figure 3F), we

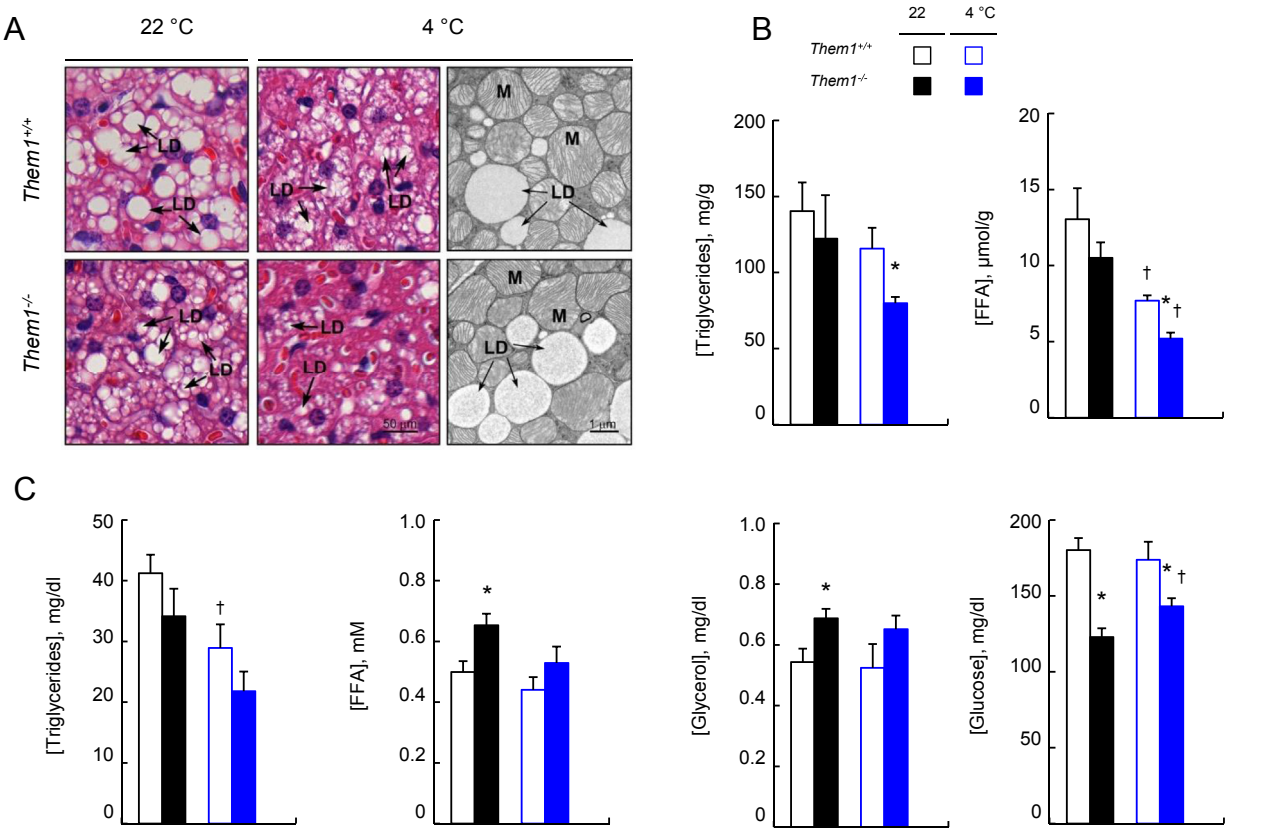

Figure 2: Effects of Them1 expression on BAT structure and on tissue and plasma concentrations of energy substrates. (A) Representative images of BAT samples subjected to hematoxylin and eosin staining and electron microscopy (abbreviations: LD, lipid droplet, M, mitochondria). (B) BAT concentrations of triglycerides and FFA. (C) Plasma concentrations of triglycerides, FFA, glycerol and glucose (n = 6/group). Error bars represent SEM. $^{*}P < 0.05$, *Them1*$^{-/-}$ vs. *Them1*$^{+/+}$ mice; $^{\dagger}P < 0.05$, 4 °C vs. 22 °C.

evaluated genotype-dependent differences at each temperature by adjusting for tissue mass. Independent of BAT mass, the absence of Them1 was associated with a significant increase in these adjusted OCR values in cold-challenged *Them1*$^{-/-}$ mice (Figure 3G). OCR values were also increased at 22 °C, but this did not achieve significance.

To understand what might be driving enhanced thermogenesis *in vivo* and elevated OCR of BAT, we examined gene expression of key BAT genes that regulate differentiation, thermogenesis, fatty acid oxidation, as well as compensation from other Acots (Table S2). Apart from reduced upregulation of *Acot8* at 4 °C in *Them1*$^{-/-}$ mice, there were no genotype-related differences suggesting non-transcriptional regulation of thermogenesis by Them1. To determine if the enhanced energy expenditure in BAT might be secondary to increased substrate availability, we assessed protein phosphorylation of Hsl and Plin1. Exposure to 4 °C tended to promote phosphorylation of Hsl at each major site, with tendencies towards reduced migration of Plin1 and upregulation of Plin1 and Atgl expression (Figure S2B). However, there were no differences attributable to Them1 expression.

3.3. Them1 reduces fatty acid oxidation in primary brown adipocytes

Primary brown adipocytes were utilized to further probe regulatory mechanisms of Them1. Unlike BAT, *ex vivo* differentiated primary brown adipocytes expressed only low levels of Them1 (Figure S3A). In these cells Ucp1 but not Them1 expression could be induced by pretreatment of brown pre-adipocytes with NE (Figure S3A). The medium concentration of FBS weakly influenced Them1 expression (Figure S3B), which was not affected by exposure to palmitate, oleate, PMA and H_2O_2 (Figure S3C). NE pretreatment increased basal OCR values, which varied linearly as a function of Ucp1 expression levels (Figure S3D). To test Them1 function, we chose 1 μM NE to pretreat cells, which led only to a 25% decrease in the triglyceride contents of brown adipocytes irrespective of Them1 expression (Figure S3E, left panel), a slight decrease in FFA concentration in the absence of Them1 expression (Figure S3E, right panel) and to modest gene expression changes that were largely independent of Them1 expression (Table S3).

Irrespective of Ucp1 induction by NE pretreatment, there were no Them1-dependent differences in basal or NE-stimulated values of OCR, which were likely due to the low levels of Them1 expression in this system (Figure 4A,B). However, when Them1 expression was reconstituted to a similar level as expressed in wild type BAT using recombinant adenovirus at a multiplicity of infection (MOI) of 40 (Figure S3F and G, and Table S3), suppression of OCR was observed: In the absence of NE pretreatment, Them1 expression did not influence basal OCR values (Figure 4C), but attenuated the increases observed following acute NE stimulation. Following NE pretreatment, Them1 but not GFP expression reduced both basal and NE-stimulated OCR values (Figure 4D). To ensure specificity, we tested the effects of similarly reconstituting Them2 (Figure S3H and I), the expression of which was more modestly reduced in primary brown adipocytes (Figure S3F). Irrespective of pretreatment with NE, expression of Them2 did not influence either basal OCR values or the response to NE stimulation in *Them1*$^{+/+}$ (Figure 4E,F) or *Them1*$^{-/-}$ (Figure S3J and K) brown adipocytes.

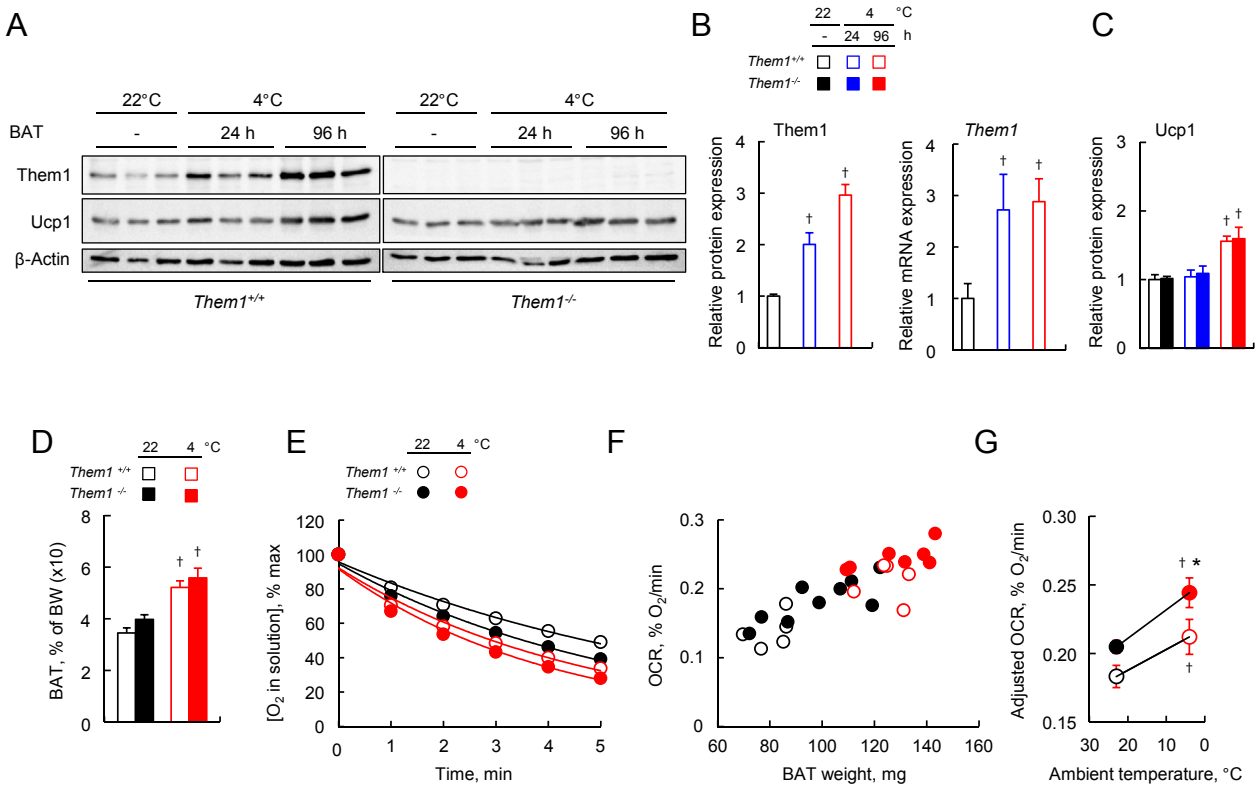

Figure 3: Ambient temperature regulates Them1 expression and OCR in BAT. (A) Them1 and Ucp1 expression in BAT homogenates. (B) Expression levels of Them1 protein relative to β-Actin and mRNA (n = 4–6/group). (C) Ucp1 protein relative to β-Actin. Freshly isolated interscapular BAT from 7 to 9 w-old mice (n = 5–9/group) analyzed for (D) BAT weight normalized by body weight, (E) O_2 concentrations expressed as % of the initial value and fit to the equation $[O_2] = 100{*}e^{-OCR{*}t}$ and (F) dependence of OCR on BAT mass. (G) OCR values were adjusted for BAT mass by ANCOVA at 22 °C and 4 °C. Error bars represent ±SEM. $^{*}P < 0.05$, *Them1*$^{-/-}$ vs. *Them1*$^{+/+}$ mice; $^{\dagger}P < 0.05$, 22 °C vs. 4 °C.

3.4. Them1 suppresses oxidation of endogenous but not exogenous fatty acids

In order to determine whether differences in OCR were attributable to the availability of endogenous fatty acids, we treated primary brown adipocytes with the carnitine palmitoyl transferase (CPT) 1 inhibitor, etomoxir (Figure 5A). OCR values in cells lacking Them1 progressively decreased to levels observed in *Them1*$^{-/-}$ brown adipocytes that were reconstituted with Them1. In the presence of etomoxir, NE stimulation only modestly increased OCR values, irrespective of Them1 expression. To further examine whether higher basal OCR values observed in the absence of Them1 were attributable to oxidation of lipid droplet-derived fatty acids, we utilized the Atgl inhibitor Atglistatin (Figure 5B). Addition of Atglistatin also reduced OCR values in GFP-expressing *Them1*$^{-/-}$ brown adipocytes to values observed in Them1-expressing cells, and eliminated the differences in response to NE stimulation. This was not attributable to lipid availability because in absence of NE pretreatment, reconstitution of Them1 expression influenced neither triglyceride nor FFA concentrations (Figure 5C). Consistent with reduced triglyceride concentrations due to NE pretreatment, rates of glycerol release were also reduced in response to acute NE stimulation (Figure 5D). However, Them1 expression did not influence glycerol release under either experimental condition, suggesting that the primary effect of Them1 was on basal OCR. We further examined phosphorylation of Hsl and Plin1, as well as expression of Atgl (Figure S4A), but observed no genotype-related differences with or without NE pretreatment.

In response to exogenous palmitate, OCR values did not differ in GFP- and Them1-reconstituted cells (Figure 5E). Moreover, oxidation of exogenous ^{14}C-palmitate into ^{14}C-ASM and ^{14}C-CO_2 was unchanged in the absence of Them1 expression (inset to Figure 5E). Similarly, expression of Them2 had no effect on the oxidation of exogenous fatty acids (Figure S4B). To examine the influence of Them1 expression on cellular mitochondrial function, primary brown adipocytes were sequentially exposed to oligomycin, FCCP, and antimycin plus rotenone, which assess ATP-linked O_2 consumption, maximum OCR, and non-mitochondrial OCR, respectively [12]. There were no differences in cellular bioenergetic parameters (Figure 5F), indicating that Them1 expression did not influence intrinsic mitochondrial function. In keeping with previous demonstrations that endogenous Them2 expression does not alter mitochondrial function in brown adipocytes [12], there were no effects of heterologous Them2 expression (Figure S4C).

4. DISCUSSION

The current findings support a function of Them1 in suppressing cold-induced thermogenesis in BAT, and the data are consistent with a model in which Them1 limits basal hydrolysis of long chain fatty acyl-CoAs, reducing mitochondrial uptake and β-oxidation (Figure 6).

In the setting of cold stress, Them1 reduced energy expenditure, and the magnitude of this effect did not diminish over time (i.e. the effect was observed under both temperature-dynamic and temperature-equilibrated conditions). Because Them1 expression was minimal in WAT and did not influence Ucp1 expression, browning of WAT might have been expected to compensate for Them1-mediated suppression of BAT thermogenesis [24,25]. However, the inhibitory effects of

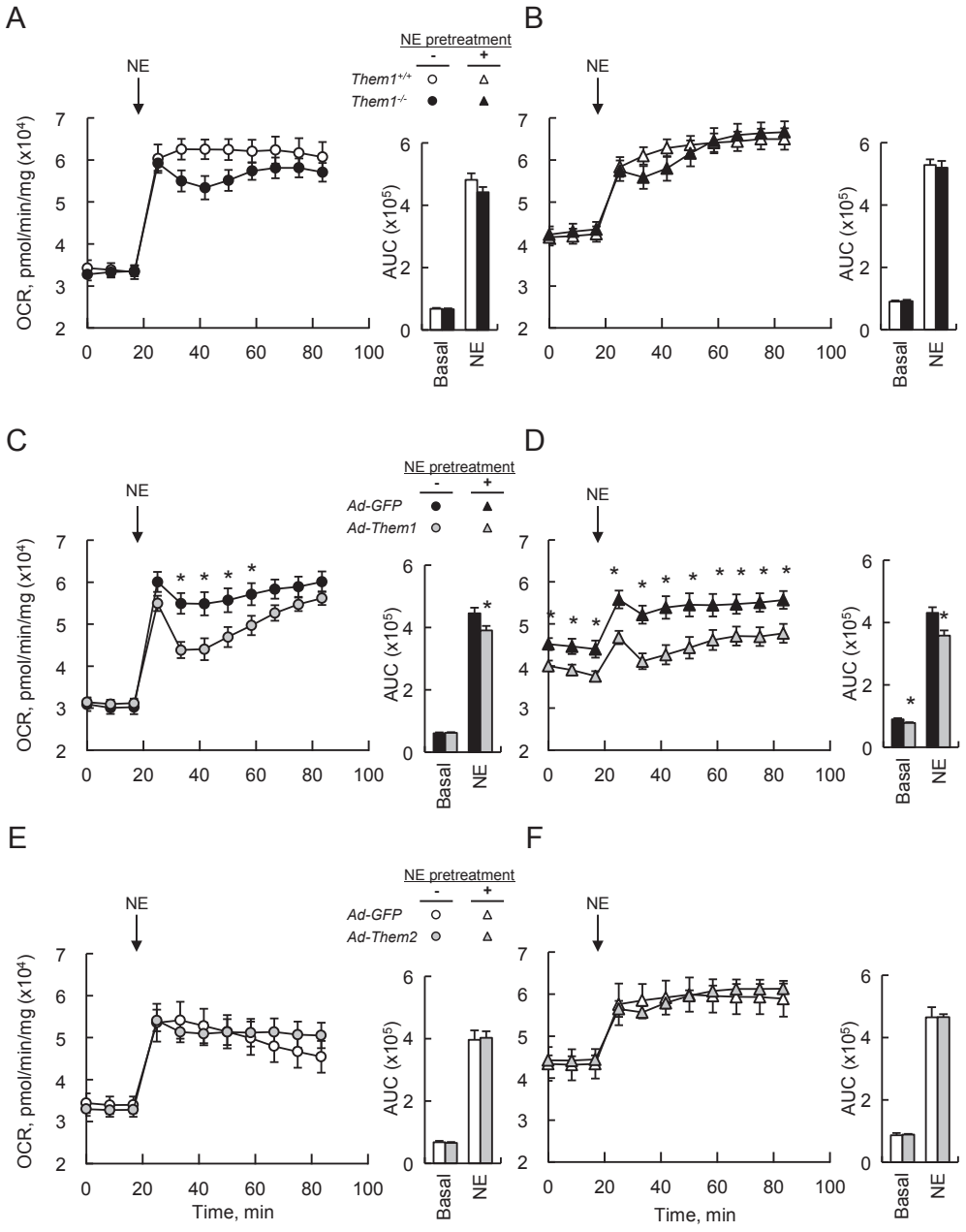

Figure 4: Them1 suppresses fatty acid oxidation in primary brown adipocytes. Response of OCR values (n = 10) to stimulation with 1 μM NE for (A,B) *Them1*$^{+/+}$ and *Them1*$^{-/-}$ brown adipocytes (data are representative of 2 independent experiments), (C,D) *Them1*$^{-/-}$ brown adipocytes reconstituted with Them1 using Ad-Them1 (MOI 40) (data are representative of 3 independent experiments) and (E,F) *Them1*$^{+/+}$ brown adipocytes reconstituted with Them2 using Ad-Them2 (MOI 40). In experiments using adenovirus, Ad-GFP (MOI 40) served as the control. The bar graphs in each panel provide basal and NE-stimulated AUC values. Error bars represent ± SEM. $^{*}P < 0.05$, *Ad-Them1* vs. *Ad-GFP*.

Them1 on energy expenditure were unabated after 96 h cold exposure, presumably reflecting the increase in Them1 expression in BAT that occurred during this period.

Consistent with an effect of Them1 on basal thermogenesis, the increased energy expenditure in *Them1*$^{-/-}$ mice at reduced ambient temperatures was most evident during the light phase. These increases were not explained by increases in physical activity or core body temperatures. Consistent with an effect restricted to non-shivering thermogenesis, increases in daily energy expenditures were not detected during the dark phase, when physical activity and food intake were maximal. However, we did observe higher values of hourly energy expenditures during the dark phase in *Them1*$^{-/-}$ mice, suggesting that basal differences were nevertheless still present in the dark.

A suppressive effect of Them1 on cold-induced thermogenesis was supported by *in vivo*, *ex vivo* and *in vitro* experiments. When taken together with increased OCR values in BAT isolated from *Them1*$^{-/-}$ mice subjected to cold stress, these observations most likely explain reduced lipid droplet abundance and decreased tissue triglyceride and FFA concentrations. The elevated plasma concentrations of FFA and glycerol and reduced glucose concentrations, as well as increased insulin sensitivity of *Them1*$^{-/-}$ mice are consistent with increased

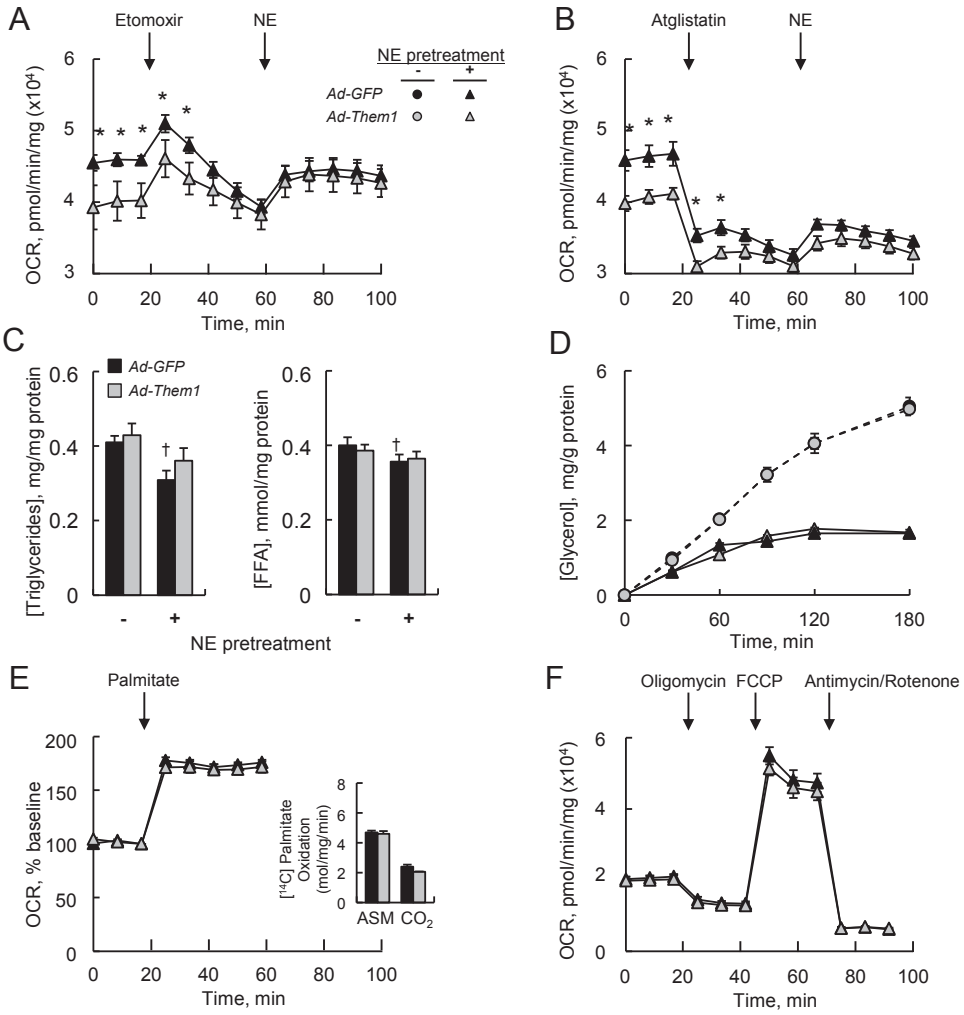

Figure 5: Them1 suppresses Atgl-dependent oxidation of endogenous fatty acids. Primary brown adipocytes from BAT of *Them1*$^{-/-}$ mice were exposed (MOI 40) to recombinant Ad-Them1 or Ad-GFP and pretreated with NE. Response of OCR values (n = 10) to the sequential addition to the media of (A) 200 μM etomoxir and 1 μM NE or (B) 40 μM Atglistatin [38] and 1 μM NE to the media (data are representative of 2 independent experiments). (C) Influence of NE pretreatment on triglyceride and FFA concentrations in primary brown adipocytes (n = 5–8/group). (D) Rates of triglyceride lipolysis (n = 3) following the addition of 1 μM NE (data representative of 2 independent experiments). Data for Ad-GFP in the absence of NE pretreatment are not visualized because they fall behind the data points for Ad-Them1. (E) Response of OCR values to 300 μM palmitate as indicated by the arrow (n = 10). Inset: Oxidation rates (n = 3) of 200 μM [1−^{14}C] palmitate. (F) Response of OCR values (n = 10) to the sequential addition of oligomycin (2 μM), FCCP (1 μM), and rotenone (1 μM) plus antimycin A (1 μM) [12]. Error bars represent ± SEM. $^{*}P < 0.05$, *Ad-Them1* vs. *Ad-GFP*; $^{\dagger}P < 0.05$, with 1 μM NE pretreatment vs no NE pretreatment.

caloric demands of BAT. Presumably because increased glucose uptake and oxidation occur in response to BAT activation [26], *Them1*$^{-/-}$ mice did not exhibit changes in RER values. Considering that 60% or more of mouse energy expenditure in the cold is attributable to BAT thermogenesis [27], the 15% increase in OCR in isolated BAT from cold exposed *Them1*$^{-/-}$ mice should be sufficient to account for the ~7% increases in cumulative daily energy expenditure observed in the intact animal. Although we did not detect an increase in body temperatures of *Them1*$^{-/-}$ mice in the setting of their higher metabolic rates, our thermography data do not support a primary thermoregulatory phenotype whereby increased heat loss served to promote accelerated metabolic fluxes in the cold [22]. Since β_3-agonist-induced increases in VO_2 at thermoneutrality are primarily attributable to activation of BAT [14,21], the much slower decline in VO_2 values for *Them1*$^{-/-}$ mice following CL316,243 injection that occurred in the absence of altered thermogenic gene expression, support a direct role for Them1 in suppressing BAT thermogenesis. Although we cannot exclude a role for Them1 in skeletal muscle fatty acid and glucose metabolism, Them1 is expressed a very low levels in skeletal muscle compared to BAT [11]. However, a BAT-specific *Them1*$^{-/-}$ mouse would be required to distinguish these possibilities with certainty.

Studies in primary BAT cells provided additional insights into a mechanistic role for Them1 in reducing oxidation of endogenous fatty acids. Increases in OCR attributable to the absence of Them1 were abrogated by inhibiting CPT1, which is rate-limiting for the mitochondrial uptake of fatty acids, or Atgl, which is the rate-limiting enzyme for lipid-droplet triglyceride hydrolysis [28]. Although its precise subcellular localization remains unknown, Them1 in BAT of mice housed at room temperature was, upon subcellular fractionation, largely concentrated in the endoplasmic reticulum (ER) [9,11], which plays critical roles in the metabolism of lipid droplets [29]. Recent studies have suggested that Them1 translocates to the lipid droplet in

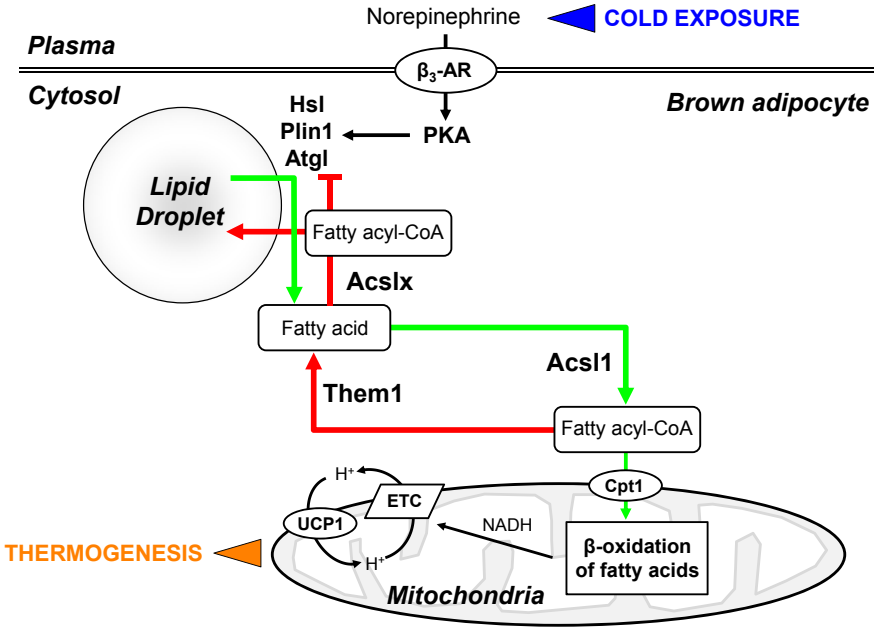

Figure 6: Schematic model of suppression of cold thermogenesis by Them1. In response to cold exposure, NE release from sympathetic neurons activates the β3-adrenergic receptor (β_3-AR), leading to activation of PKA. PKA in turn stimulates lipolysis by phosphorylation of Plin1, which leads to activation of Atgl, the rate-limiting step in lipid droplet triglyceride hydrolysis. PKA also phosphorylates and activates Hsl. FFA liberated as a result of lipolysis are the activated by Acsl1 and taken up into mitochondrial by the activity of carnitine palmitoyl transferase 1 (Cpt1). The proton-gradient generated by the activity of the electron transport chain following β-oxidation of fatty acids is uncoupled from ATP synthesis by Ucp1. Them1 opposes the activity of Acsl1, generating FFA that are then converted by an as yet identified Acsl (i.e. Acslx), which suppress activity of Atgl and may be reassembled into triglycerides for lipid droplet storage.

the setting of lipolytic stimulation. A proteomic analysis of BAT lipid droplets isolated from mice exposed to the 4 °C compared with mice housed at room temperature revealed the association of Them1 with lipid droplets, along with a 2.5-fold enrichment following cold exposure [30]. The same analysis revealed cold-mediated enrichment of BAT lipid droplets with both HSL and ATGL. We visualized cold-induced relocation of Them1 to BAT lipid droplets by colocalization with Plin1, and this was validated with immunoblot analysis of isolated lipid droplets [31]. As a result, Them1 may be well positioned to regulate lipolysis by generating FFA in close proximity to lipid droplets under lipolytic conditions.

Whereas Atgl activity is only modestly suppressed by FFA, fatty acyl-CoAs are potent non-competitive inhibitors [32]. This suggests that Atgl may be inhibited when Them1-generated FFA are converted locally with fatty acyl-CoAs. Indeed, considerable evidence suggests that FFA esterification to CoASH is compartmentalized by Acsl isoforms that are regionally distributed within cells [33]. Whereas Acsl1 promotes mitochondrial fatty acyl-CoA uptake [34], a distinct Acsl (represented as Acslx in Figure 6) presumably generates fatty acyl-CoAs that both inhibit Atgl and serve as substrates for lipid droplet triglycerides. Because this model depends in part on the use of pharmacologic inhibitors, it should be strengthened by corresponding genetic gain- and loss-of function studies, as well as to the Acslx once it is identified.

Because the enzymatic activity of Them1 contributes to the overall balance of FFA and fatty acyl-CoAs in BAT [9,11], another potential mechanism by which it could regulate thermogenesis in BAT is via peroxisome proliferator-activated receptor (Ppar) activation [1]. This was unlikely because we did not observe Them1-dependent changes in mRNA levels of Ppar targets or of other key thermogenic genes, including Acsl1 and Fabp3, which function to promote fatty acid oxidation within BAT [34,35]. The absence of changes in expression levels of a broad panel of regulatory genes supports a non-transcriptional mechanism whereby Them1 suppresses cold thermogenesis.

The absence of Them1 upregulation by β_3-adrenergic stimulation *in vivo* or by NE pretreatment of primary brown adipocytes suggests that the transcriptional regulation of Them1 by ambient temperature may occur by a mechanism distinct from the cold-driven transcriptional thermogenic program of BAT [36]. However, Them1 expression was not restored in response to exogenous FFA, serum or reactive oxygen species in the form of H_2O_2. Protein kinase C (PKC) β can suppress thermogenesis [37], but a PKC activator did not reconstitute Them1 expression. As evidenced by an increase in protein expression following prolonged cold exposure that was unaccompanied by increases in mRNA levels, Them1 upregulation also appears to involve post-translational effects. The mechanisms by which cold exposure upregulates Them1 expression require further investigation.

Taken together, our findings suggest the presence of an active feedback mechanism that limits cold thermogenesis in BAT even in the setting of a prolonged cold stress. This likely underscores the survival value of energy conservation, such that the calorie intensive process of non-shivering thermogenesis is rapidly suppressed when no longer necessary. Because it reduces thermogenesis in proportion to its expression level and without broadly altering gene expression, Them1 may represent an attractive target for management of obesity and related metabolic disorders.

AUTHOR CONTRIBUTIONS

Author contributions: K.O. and D.E.C. designed research; K.O., K.B.L., Y.Z., Y.L., T.I.K., C.O. and S.J.H. performed research; K.O., K.B.L., S.J.H., T.I.K., R.A.B., A.S.B. and D.E.C. analyzed data; and K.O., A.S.B. and D.E.C. wrote the paper.

ACKNOWLEDGMENTS

This work was supported by U.S. National Institutes of Health grants R01 DK056626 and R37 DK048873 (to D.E.C.), R01 DK103046 (to D.E.C. and S.J.H.) the Harvard Digestive Diseases Center (P30 DK034854) and the Harvard Catalyst, support by the National Center for Advancing Translational Sciences (UL1 TR001102).

CONFLICT OF INTEREST

None declared.

APPENDIX A. SUPPLEMENTARY DATA

Supplementary data related to this article can be found at http://dx.doi.org/10.1016/j.molmet.2016.02.002.

REFERENCES

[1] Cannon, B., Nedergaard, J., 2004. Brown adipose tissue: function and physiological significance. Physiological Reviews 84:277–359.
[2] Ellis, J.M., Frahm, J.L., Li, L.O., Coleman, R.A., 2010. Acyl-coenzyme A synthetases in metabolic control. Current Opinion in Lipidology 21:212–217.
[3] Kajimura, S., Seale, P., Spiegelman, B.M., 2010. Transcriptional control of brown fat development. Cell Metabolism 11:257–262.
[4] Sidossis, L., Kajimura, S., 2015. Brown and beige fat in humans: thermogenic adipocytes that control energy and glucose homeostasis. Journal of Clinical Investigation 125:478–486.
[5] Adams, S.H., Chui, C., Schilbach, S.L., Yu, X.X., Goddard, A.D., Grimaldi, J.C., et al., 2001. BFIT, a unique acyl-CoA thioesterase induced in thermogenic brown adipose tissue: cloning, organization of the human gene and assessment of a potential link to obesity. Biochemical Journal 360:135–142.
[6] Brocker, C., Carpenter, C., Nebert, D.W., Vasiliou, V., 2010. Evolutionary divergence and functions of the human acyl-CoA thioesterase gene (ACOT) family. Human Genomics 4:411–420.
[7] Kirkby, B., Roman, N., Kobe, B., Kellie, S., Forwood, J.K., 2010. Functional and structural properties of mammalian acyl-coenzyme A thioesterases. Progress in Lipid Research 49:366–377.
[8] Chen, D., Latham, J., Zhao, H., Bisoffi, M., Farelli, J., Dunaway-Mariano, D., 2012. Human brown fat inducible thioesterase variant 2 cellular localization and catalytic function. Biochemistry 51:6990–6999.
[9] Han, S., Cohen, D.E., 2012. Functional characterization of thioesterase superfamily member 1/Acyl-CoA thioesterase 11: implications for metabolic regulation. Journal of Lipid Research 53:2620–2631.
[10] Lau, P., Tuong, Z.K., Wang, S.C., Fitzsimmons, R.L., Goode, J.M., Thomas, G.P., et al., 2015. Roralpha deficiency and decreased adiposity are associated with induction of thermogenic gene expression in subcutaneous white adipose and brown adipose tissue. American Journal of Physiology Endocrinology and Metabolism 308:E159–E171.
[11] Zhang, Y., Li, Y., Niepel, M.W., Kawano, Y., Han, S., Liu, S., et al., 2012. Targeted deletion of thioesterase superfamily member 1 promotes energy expenditure and protects against obesity and insulin resistance. Proceedings of the National Academy of Sciences of the United States of America 109:5417–5422.
[12] Kang, H.W., Ozdemir, C., Kawano, Y., LeClair, K.B., Vernochet, C., Kahn, C.R., et al., 2013. Thioesterase superfamily member 2/Acyl-CoA thioesterase 13 (Them2/Acot13) regulates adaptive thermogenesis in mice. Journal of Biological Chemistry 288:33376–33386.
[13] Tschop, M.H., Speakman, J.R., Arch, J.R., Auwerx, J., Bruning, J.C., Chan, L., et al., 2012. A guide to analysis of mouse energy metabolism. Nature Methods 9:57–63.
[14] Poggioli, R., Ueta, C.B., Drigo, R.A., Castillo, M., Fonseca, T.L., Bianco, A.C., 2013. Dexamethasone reduces energy expenditure and increases susceptibility to diet-induced obesity in mice. Obesity (Silver Spring) 21:E415–E420.
[15] Crane, J.D., Mottillo, E.P., Farncombe, T.H., Morrison, K.M., Steinberg, G.R., 2014. A standardized infrared imaging technique that specifically detects UCP1-mediated thermogenesis in vivo. Molecular Metabolism 3:490–494.
[16] Petrovic, N., Shabalina, I.G., Timmons, J.A., Cannon, B., Nedergaard, J., 2008. Thermogenically competent nonadrenergic recruitment in brown preadipocytes by a PPARgamma agonist. American Journal of Physiology Endocrinology and Metabolism 295:E287–E296.
[17] Kang, H.W., Ribich, S., Kim, B.W., Hagen, S.J., Bianco, A.C., Cohen, D.E., 2009. Mice lacking phosphatidylcholine transfer protein/StarD2 exhibit increased adaptive thermogenesis and enlarged mitochondria in brown adipose tissue. Journal of Lipid Research 50:2212–2221.
[18] Kawano, Y., Ersoy, B.A., Li, Y., Nishiumi, S., Yoshida, M., Cohen, D.E., 2014. Thioesterase superfamily member 2 (Them2) and phosphatidylcholine transfer protein (PC-TP) interact to promote fatty acid oxidation and control glucose utilization. Molecular and Cellular Biology 34:2396–2408.
[19] Rybin, V.O., Guo, J., Gertsberg, Z., Feinmark, S.J., Steinberg, S.F., 2008. Phorbol 12-myristate 13-acetate-dependent protein kinase C delta-Tyr311 phosphorylation in cardiomyocyte caveolae. Journal of Biological Chemistry 283:17777–17788.
[20] Xu, B., Zhang, J., Strom, J., Lee, S., Chen, Q.M., 2014. Myocardial ischemic reperfusion induces de novo Nrf2 protein translation. Biochimica et Biophysica Acta 1842:1638–1647.
[21] Cannon, B., Nedergaard, J., 2011. Nonshivering thermogenesis and its adequate measurement in metabolic studies. Journal of Experimental Biology 214:242–253.
[22] Sampath, H., Ntambi, J.M., 2014. Role of stearoyl-CoA desaturase-1 in skin integrity and whole body energy balance. Journal of Biological Chemistry 289:2482–2488.
[23] Lee, J., Ellis, J.M., Wolfgang, M.J., 2015. Adipose fatty acid oxidation is required for thermogenesis and potentiates oxidative stress-induced inflammation. Cell Reports 10:266–279.
[24] Guerra, C., Koza, R.A., Yamashita, H., Walsh, K., Kozak, L.P., 1998. Emergence of brown adipocytes in white fat in mice is under genetic control. Effects on body weight and adiposity. Journal of Clinical Investigation 102:412–420.
[25] Xue, B., Coulter, A., Rim, J.S., Koza, R.A., Kozak, L.P., 2005. Transcriptional synergy and the regulation of Ucp1 during brown adipocyte induction in white fat depots. Molecular and Cellular Biology 25:8311–8322.
[26] Cannon, B., Nedergaard, J., 2010. Metabolic consequences of the presence or absence of the thermogenic capacity of brown adipose tissue in mice (and probably in humans). International Journal of Obesity (London) 34:S7–S16.
[27] Virtue, S., Vidal-Puig, A., 2013. Assessment of brown adipose tissue function. Frontiers in Physiology 4:128.
[28] Lass, A., Zimmermann, R., Oberer, M., Zechner, R., 2011. Lipolysis – a highly regulated multi-enzyme complex mediates the catabolism of cellular fat stores. Progress in Lipid Research 50:14–27.
[29] Walther, T.C., Farese Jr., R.V., 2012. Lipid droplets and cellular lipid metabolism. Annual Review of Biochemistry 81:687–714.
[30] Yu, J., Zhang, S., Cui, L., Wang, W., Na, H., Zhu, X., et al., 2015. Lipid droplet remodeling and interaction with mitochondria in mouse brown adipose tissue during cold treatment. Biochimica et Biophysica Acta 1853:918–928.
[31] Li, Y., Hagen, S.J., Cohen, D.E., 2015. Tissue-specific subcellular localization of thioesterase superfamily member 1 (Them1) in the pathogenesis of nonalcoholic fatty liver disease (NAFLD) (abstract). Hepatology 62:374A.
[32] Nagy, H.M., Paar, M., Heier, C., Moustafa, T., Hofer, P., Haemmerle, G., et al., 2014. Adipose triglyceride lipase activity is inhibited by long-chain acyl-coenzyme A. Biochimica et Biophysica Acta 1841:588–594.

[33] Cooper, D.E., Young, P.A., Klett, E.L., Coleman, R.A., 2015. Physiological consequences of compartmentalized acyl-CoA metabolism. Journal of Biological Chemistry 290:20023–20031.

[34] Ellis, J.M., Li, L.O., Wu, P.C., Koves, T.R., Ilkayeva, O., Stevens, R.D., et al., 2010. Adipose acyl-CoA synthetase-1 directs fatty acids toward beta-oxidation and is required for cold thermogenesis. Cell Metabolism 12: 53–64.

[35] Vergnes, L., Chin, R., Young, S.G., Reue, K., 2011. Heart-type fatty acid-binding protein is essential for efficient brown adipose tissue fatty acid oxidation and cold tolerance. Journal of Biological Chemistry 286:380–390.

[36] Seale, P., Kajimura, S., Spiegelman, B.M., 2009. Transcriptional control of brown adipocyte development and physiological function–of mice and men. Genes & Development 23:788–797.

[37] Mehta, N.K., Mehta, K.D., 2014. Protein kinase C-beta: an emerging connection between nutrient excess and obesity. Biochimica et Biophysica Acta 1841:1491–1497.

[38] Li, Y., Fromme, T., Schweizer, S., Schottl, T., Klingenspor, M., 2014. Taking control over intracellular fatty acid levels is essential for the analysis of thermogenic function in cultured primary brown and brite/beige adipocytes. EMBO Reports 15:1069–1076.

